

Density functional calculations and analysis of the crystal structure of $\text{Pb}_2\text{P}_2\text{O}_7$

M. Siewattana

*Materials Science and Technology Division, Oak Ridge National Laboratory, Oak Ridge, Tennessee 37831-6032, USA
and Department of Physics, University of Tennessee, Knoxville, Tennessee 37996-1200, USA*

D. J. Singh

Materials Science and Technology Division, Oak Ridge National Laboratory, Oak Ridge, Tennessee 37831-6032, USA

M. Fornari

*Department of Physics, Central Michigan University, Mt. Pleasant, Michigan 48859, USA
(Received 21 February 2007; revised manuscript received 4 April 2007; published 22 May 2007)*

Density functional calculations of the atomic coordinates in crystalline lead pyrophosphate ($\text{Pb}_2\text{P}_2\text{O}_7$) are reported. These calculations yield atomic positions differing from a prior x-ray refinement by up to 0.2 Å. The main difference is a change in the orientation of the $(\text{P}_2\text{O}_7)^{4-}$ units to bring certain O ions closer to Pb. An analysis of the resulting structure in terms of pair distribution functions is presented. These show that the most significant changes are in the local Pb coordination. The electronic structure is not significantly affected by the change in crystal structure.

DOI: [10.1103/PhysRevB.75.172105](https://doi.org/10.1103/PhysRevB.75.172105)

PACS number(s): 61.18.-j, 71.15.Nc, 71.55.Ht

Phosphate crystals and glasses are of interest for several reasons. Activated orthophosphates (e.g., $\text{LuPO}_4:\text{Ce}$) are useful scintillators for γ - and x-ray detection.¹ Phosphate catalysts, based on vanadyl phosphate, are widely used in the chemical industry. The combination of high optical quality, chemical stability, and radiation hardness found in many phosphate glasses makes them amenable to applications ranging from optical elements to forms for long-term storage of radioactive waste.^{2,3} These materials have flexible saltlike structures composed of very strongly bonded anionic phosphate groups or pyrophosphate chains (these are phosphate groups linked by shared O) and cations in the interstices. Orthophosphates [compounds based on $(\text{PO}_4)^{3-}$] are typically crystalline, while materials based on longer phosphate chains often form glasses. Such glasses activated by appropriate luminescent centers are used as active laser elements, and there is current interest in the use of activated phosphate glasses as scintillators for radiation detection. As mentioned, many crystalline phosphates are good scintillators when activated, typically with rare-earth metals (especially Ce^{3+}). However, effective activation of phosphate glasses to obtain light yields comparable to high-quality crystalline materials has yet to be reported. Microscopic understanding of the structural differences between the various phosphate crystals and corresponding glasses may be helpful in formulating strategies for making good phosphate glass scintillators.

Lead pyrophosphate $\text{Pb}_2\text{P}_2\text{O}_7$ is a particularly interesting compound because it forms a line compound with a well-ordered crystalline phase when cooled normally, but forms a bulk glass when cooled quickly from melt. The structure of the glass phase is not known in detail, although it is known that it is essentially different from the types of structure that can be formed by amorphizing the crystalline form using radiation damage⁴ and that the distribution of phosphate chain lengths differs from the crystalline form,⁵ in which all chains have length 2: i.e., $(\text{P}_2\text{O}_7)^{4-}$. The crystalline form is triclinic and micaceous. The crystal structure was determined

by Mullica and co-workers⁶ in 1986 using Mo $K\alpha$ x-ray diffraction. They found a complex structure, spacegroup $P1$, with 44 atoms per unit cell, all of which are on general sites: 4 inequivalent Pb, 4 inequivalent P, and 14 inequivalent O positions, for a total of 66 internal coordinates. Refinement of such a structure by x-ray diffraction is extremely difficult, especially considering the combination of Pb and O, which have very different x-ray scattering cross sections. A similar challenge was presented by the structure of PbZrO_3 , which has a 40-atom orthorhombic cell. In that case, structural relaxations using density functional calculations were helpful. In particular, local density approximation (LDA) calculations yielded a structure with different O coordinates than the accepted experimental structure,⁷ but were confirmed by subsequent neutron experiments that yielded a crystal structure in close agreement with the LDA structure.^{8,9} It was noted in recent LDA calculations of the electronic properties of various phosphates,¹⁰ including $\text{Pb}_2\text{P}_2\text{O}_7$, done with experimental crystal structures, that the forces on some atoms in this material were substantial. The largest of these was $\sim 0.17 \text{ Ry}/a_0$ on the O(5) atom and $\sim 0.15 \text{ Ry}/a_0$ on the P(2) atom, using the notation of Ref. 6. These forces are larger than those normally found in LDA calculations for non-transition-element-containing oxides with experimental crystal structures.

The present paper presents calculations of the structure of $\text{Pb}_2\text{P}_2\text{O}_7$. These were done by relaxing the internal coordinates of all inequivalent atoms in the unit cell using the calculated LDA forces. The lattice parameters were held fixed at their experimental values $a=6.941 \text{ Å}$, $b=6.966 \text{ Å}$, $c=12.751 \text{ Å}$, $\alpha=96.82^\circ$, $\beta=91.14^\circ$, and $\gamma=89.64^\circ$ and triclinic $P1$ spacegroup, as determined by Mullica and co-workers.⁶ These are obtained experimentally from the positions of the Bragg peaks and are no doubt much more accurate than values that can be obtained from LDA calculations. The structure relaxation was done using the general potential linearized augmented plane-wave (LAPW) method,

TABLE I. Atomic positions in lattice coordinates of $\text{Pb}_2\text{P}_2\text{O}_7$ from x-ray diffraction (Ref. 6), LAPW structural relaxation, and the difference between experimental and calculated positions ΔR (in Å). The notation is as in Ref. 6.

Atoms	X-ray			Relaxed			ΔR
	x	y	z	x	y	z	
Pb(1)	0.246	0.205	0.650	0.245	0.198	0.644	0.09
Pb(2)	0.673	0.211	0.860	0.668	0.217	0.860	0.06
Pb(3)	0.091	0.811	0.853	0.087	0.819	0.860	0.10
Pb(4)	0.652	0.624	0.633	0.650	0.624	0.631	0.04
P(1)	0.233	0.897	0.400	0.237	0.891	0.397	0.06
P(2)	0.185	0.698	0.590	0.184	0.697	0.589	0.01
P(3)	0.835	0.699	0.086	0.833	0.698	0.087	0.02
P(4)	0.579	0.707	0.899	0.583	0.715	0.897	0.07
O(1)	0.087	0.920	0.313	0.093	0.900	0.307	0.15
O(2)	0.391	0.763	0.361	0.412	0.766	0.360	0.15
O(3)	0.305	0.089	0.464	0.295	0.084	0.458	0.10
O(4)	0.112	0.787	0.485	0.119	0.772	0.478	0.14
O(5)	0.017	0.636	0.641	0.998	0.646	0.640	0.15
O(6)	0.300	0.855	0.657	0.306	0.855	0.651	0.09
O(7)	0.313	0.525	0.548	0.315	0.520	0.563	0.20
O(8)	0.992	0.819	0.043	0.998	0.824	0.054	0.15
O(9)	0.919	0.535	0.138	0.907	0.522	0.134	0.13
O(10)	0.700	0.830	0.155	0.694	0.832	0.153	0.05
O(11)	0.706	0.608	0.987	0.714	0.613	0.981	0.10
O(12)	0.704	0.854	0.855	0.706	0.872	0.857	0.13
O(13)	0.402	0.797	0.955	0.401	0.797	0.951	0.05
O(14)	0.525	0.539	0.818	0.548	0.547	0.812	0.19

with local orbital extensions.^{11,12} This is an all-electron method, with no shape approximations to the potential or charge density and a flexible basis set in all regions of space. As such, it is well suited to complex open structures, like that of $\text{Pb}_2\text{P}_2\text{O}_7$. Core states were treated relativistically, while valence states were treated in a scalar relativistic approximation, similar to our prior studies of PbZrO_3 .^{7,9} The calculations were done using LAPW sphere radii of $2.1a_0$, $1.38a_0$ and $1.33a_0$ for Pb, P, and O, respectively. Well-converged basis sets consisting of more than 10 300 LAPW functions plus local orbitals were employed. The relaxation was done starting from the structure of Mullica and co-workers and using a single \mathbf{k} point for the Brillouin zone sampling. When finished, the structure was checked by calculating the forces with a set of four special \mathbf{k} points. The largest force in this calculation was ~ 0.02 Ry/bohr. We also performed pseudo-potential calculations of the forces in this structure, both in the LDA and with the generalized gradient approximation (GGA) of Perdew, Burke, and Ernzerhof (PBE),¹³ but found similarly small forces. This agreement between the LDA and GGA structures is significant in view of the trend that LDA calculations underestimate bond lengths in light-atom solids, while GGA calculations yield longer bond lengths that are often, but not always in better agreement with experiment. The trends for molecules are often different, so that in light-element molecules the LDA sometimes overestimates bond

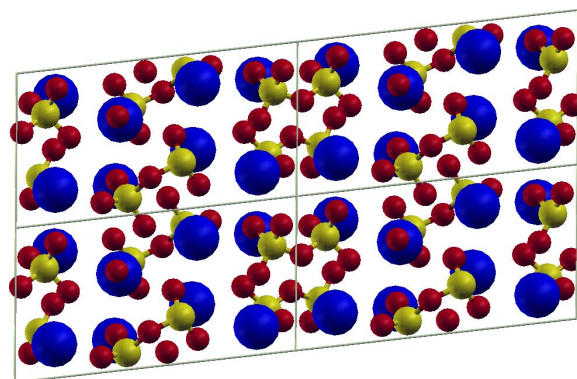


FIG. 1. (Color online) Relaxed crystal structure of triclinic $\text{Pb}_2\text{P}_2\text{O}_7$, viewed along the a axis. Pb, P, and O are depicted by large blue, medium green, and small red spheres, respectively. The light gray lines denote the unit cell.

lengths, while GGAs often improve these values.^{14,15} Both the GGA and LDA stress tensors were nearly diagonal and isotropic (to within 10% for the GGA and 5% for the LDA). The corresponding pressures were -109 kbar (LDA) and -24 kbar (GGA). These values are consistent with normal LDA and GGA errors and support the experimental lattice parameters, which as mentioned follow directly from the positions of the diffraction lines and are no doubt accurate.

Table I gives our calculated internal coordinates for $\text{Pb}_2\text{P}_2\text{O}_7$ along side the prior x-ray structure. As may be seen, there are significant shifts of 0.1 Å and more in the positions of many atoms. The final structure is shown in Fig. 1. Qualitatively, it is as described in Ref. 6. The calculated total energy of the relaxed structure, as determined from the calculations with four special \mathbf{k} points, was 21 mRy per cell (73 meV per formula unit) lower in energy than that obtained with the structure of Ref. 6. On a per atom basis, this is of the same order as the energy difference between the relaxed and prior experimental structures for PbZrO_3 (8 meV per atom in that case),⁷ although it should be noted that $\text{Pb}_2\text{P}_2\text{O}_7$ has shorter stiffer bonds than PbZrO_3 .

Structural information for glasses is normally available only in the form of pair distribution functions (PDFs). Analysis in terms of PDFs is also convenient for complex crystals.

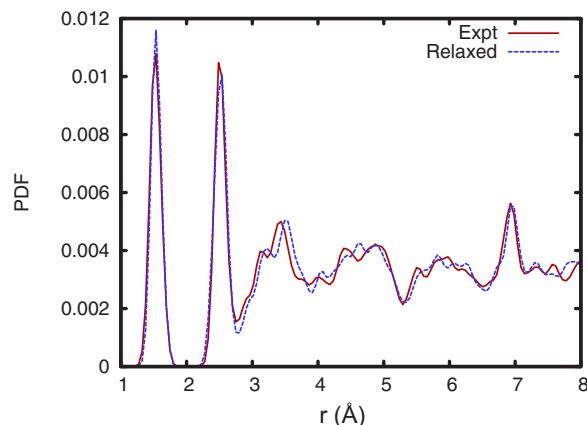


FIG. 2. (Color online) Total PDFs for the experimental and relaxed structures.

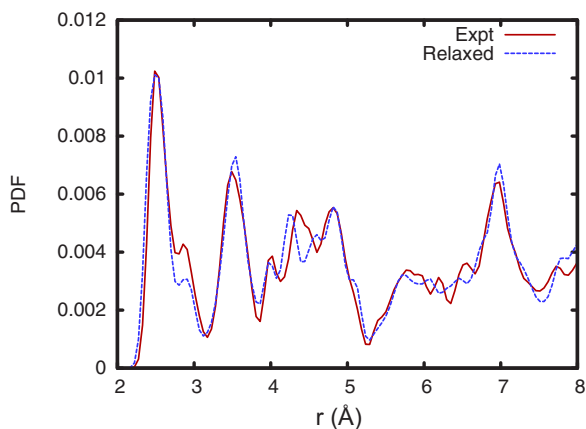


FIG. 3. (Color online) Pb PDFs with respect to all other atoms for the x-ray and relaxed structures.

Although, to our knowledge, there are no PDF structural data for $\text{Pb}_2\text{P}_2\text{O}_7$ glass, we present the PDFs for crystalline $\text{Pb}_2\text{P}_2\text{O}_7$ both to compare the x-ray and LDA structures and to provide a reference for comparison with the PDF of the glass when it becomes available. The total PDF and PDFs as a function of distance for Pb, P, and O with respect to all other atoms in the lattice are shown in Figs. 2–5, respectively. These were calculated from the structure with a broadening factor of 0.1 Å. It is interesting to note that the magnitudes of the PDF for P and O with the x-ray and relaxed structures are very similar for the first- and second-neighbor shells, but that the difference is more pronounced for larger distances. On the other hand, for Pb the distortion is visible throughout the PDF profile, for example, in the second peak showing a lengthening of the nearest-neighbor distance. This comparison reflects the fact that the LDA relaxed structure differs from the experimental structure mainly by a change in the direction out of the stacking plane of pyrophosphate (or diphosphate) groups with respect to the experimental positions; there are rather small changes in P-O nearest-neighbor distances within pyrophosphate layers. As may be seen in the PDF, the main difference between the two structures is a redistribution of the neighboring O around Pb to have a narrower bond length distribution and shorter average Pb-O dis-

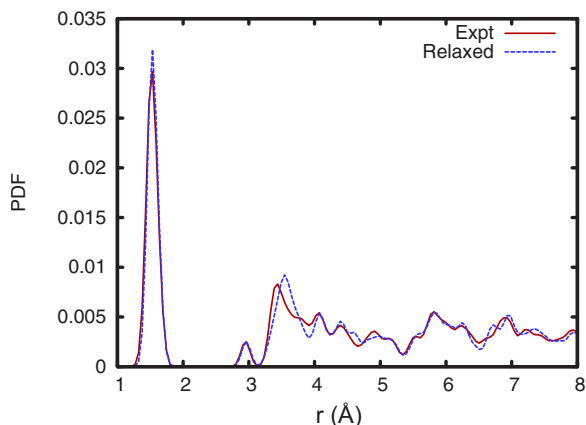


FIG. 4. (Color online) P PDF with x-ray and relaxed structures, as in Fig. 3.

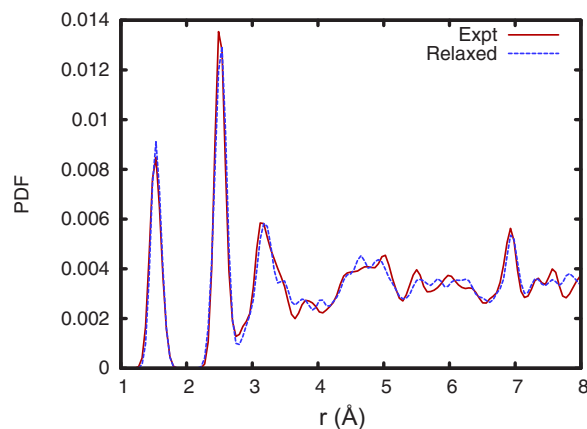


FIG. 5. (Color online) O PDF, as in Fig. 3.

tance. The other main change is a shift in the bridging O of $(\text{P}_2\text{O}_7)^{4-}$ groups, which makes it such that the two bonds become practically equal in length.

It may be noted that the structure has very short Pb-O and O-O distances. In the relaxed structure the shortest Pb-O bond is 2.384 Å, while the shortest O-O bond is 2.418 Å. The x-ray values are similar: 2.460 Å and 2.428 Å, respectively. Such short bond lengths would be highly unusual in an ionic material like PbZrO_3 and reflect the chemistry of phosphates, in particular the fact that these are salts of Pb with very strongly covalently bonded pyrophosphate groups. In comparison, lead orthophosphate, $\text{Pb}_3(\text{PO}_4)_2$, has a minimum Pb-O distance of 2.38 Å, based on the neutron structure of Angel and co-workers.¹⁶ $\text{Sr}_2\text{P}_2\text{O}_7$ has a reported minimum Sr-O distance of 2.39 Å.¹⁷ (N.B. The ionic radius of Sr^{2+} is very similar to that of Pb^{2+} .) The internal structure of the $(\text{P}_2\text{O}_7)^{4-}$ groups is very similar between the two structures and with other pyrophosphates. The minimum O-O distances are 2.487 Å in $\text{Sr}_2\text{P}_2\text{O}_7$ (Ref. 18), 2.451 Å in $(\text{VO})_2\text{P}_2\text{O}_7$ (Ref. 19), 2.438 Å in $\alpha\text{-Ca}_2\text{P}_2\text{O}_7$ (Ref. 20), 2.398 Å in $\beta\text{-Ca}_2\text{P}_2\text{O}_7$ (Ref. 21), and 2.454 Å in $\text{Na}_4\text{P}_2\text{O}_7$ (Ref. 22). The calculated structure also shares similarly bent P-O-P pyrophosphate bridges. The bond angles are 131.3° and 132.8°

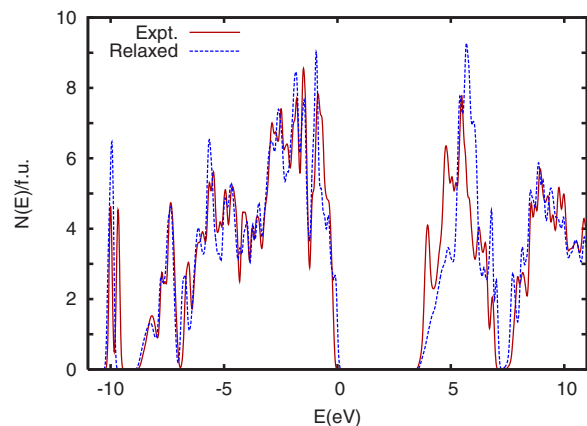


FIG. 6. (Color online) Calculated electronic density of states (per formula unit, both spins) for $\text{Pb}_2\text{P}_2\text{O}_7$ with the x-ray (Ref. 6, denoted Expt.) and relaxed atomic positions. The zero is at the valence-band edge. A Gaussian broadening of 0.08 eV was applied.

for the relaxed structure, as compared to 130.4° and 132.0° in the x-ray structure. For comparison the P-O-P bond angle in $\text{Sr}_2\text{P}_2\text{O}_7$ is 130.4° (Ref. 18).

Next we compare the electronic structure based on the density of states (DOS). The calculated DOS for the experimental and relaxed structures is given in Fig. 6. As may be seen, these are very similar in their large-scale features and the gaps and shapes of the DOS at the valence- and conduction-band edges are almost the same. The DOS reflects the bonding and chemical makeup of the compound.¹⁰ Examining the DOS in more detail, we note four visible energy manifolds, two of which are valence and two are conduction bands. In both cases, there are very narrow states appearing at the lower energy (roughly at 10 eV). These are from the symmetric bonding states of the pyrophosphate units. This involves the $p\sigma$ orbital of the O bridging the two P atoms in the pyrophosphate units, hybridized with P orbitals (but note that the P-O-P bond is bent away by 180°). The occupied states come from bonding orbitals of the pyrophosphate anion, with the σ -bonding orbitals in the lower-energy region, while the states near the valence-band edge come

from O π orbitals. The conduction manifold derives from Pb $6p$ states, while the higher-energy (above ~ 7 eV) conduction manifold is from antibonding states of the pyrophosphate group. It is not surprising that a structural change that affects mainly the orientation of the pyrophosphate will not have a large effect on the large scale structure of the DOS.

To summarize, we present a structure for $\text{Pb}_2\text{P}_2\text{O}_7$ based on LDA relaxation. This differs from the prior x-ray structure of Mullica and co-workers by shifts in the atomic positions of as much as 0.2 \AA , the difference consisting mainly of changes in the orientation of the pyrophosphate groups. These changes have only minor effects on the electronic structure, but are clearly visible in the PDF, especially in the coordination of the Pb atoms. This PDF provides a reference that can be used to compare with the PDF of glass when it is measured.

We are grateful for helpful discussions with L.A. Boatner and B.C. Sales. Work at ORNL was supported by DOE, NA22. Work at the University of Tennessee was supported by the ONR.

¹L. A. Boatner, L. A. Keefer, J. M. Farmer, D. Wisniewski, and A. J. Wojtowicz, Proc. SPIE **5540**, 73 (2004) and references therein.

²B. C. Sales and L. A. Boatner, Mater. Lett. **2**, 301 (1984).

³W. F. Krupke, M. D. Shinn, T. A. Kirchoff, C. B. Finch, and L. A. Boatner, Appl. Phys. Lett. **51**, 2186 (1987).

⁴B. C. Sales, J. O. Ramey, L. A. Boatner, and J. C. McCallum, Phys. Rev. Lett. **62**, 1138 (1989).

⁵B. C. Sales, J. O. Ramey, and L. A. Boatner, Phys. Rev. Lett. **59**, 1718 (1987).

⁶D. F. Mullica, H. O. Perkins, D. A. Grossie, L. A. Boatner, and B. C. Sales, J. Solid State Chem. **62**, 371 (1986) The value of the a lattice parameter given in the abstract differs from that in the text. The value in the text appears to be correct based on the cell volume and is what is used here.

⁷D. J. Singh, Phys. Rev. B **52**, 12559 (1995).

⁸H. Fujishita and S. Katano, J. Phys. Soc. Jpn. **66**, 3484 (1997).

⁹M. D. Johannes and D. J. Singh, Phys. Rev. B **71**, 212101 (2005).

¹⁰D. J. Singh, G. E. Jellison, Jr., and L. A. Boatner, Phys. Rev. B **74**, 155126 (2006).

¹¹D. J. Singh and L. Nordstrom, *Planewaves, Pseudopotentials and*

the LAPW Method, 2nd ed. (Springer, Berlin, 2006).

¹²D. Singh, Phys. Rev. B **43**, 6388 (1991).

¹³J. P. Perdew, K. Burke, and M. Ernzerhof, Phys. Rev. Lett. **77**, 3865 (1996).

¹⁴A. Khein, D. J. Singh, and C. J. Umrigar, Phys. Rev. B **51**, 4105 (1995).

¹⁵V. N. Staroverov, G. E. Scuseria, J. Tao, and J. P. Perdew, J. Chem. Phys. **119**, 12129 (2003).

¹⁶R. J. Angel, U. Bismayer, and W. G. Marshall, J. Phys.: Condens. Matter **13**, 5353 (2001).

¹⁷R. D. Shannon, Acta Crystallogr., Sect. A: Cryst. Phys., Diffr., Theor. Gen. Crystallogr. **32**, 751 (1976).

¹⁸J. Barbier and J. P. Echard, Acta Crystallogr., Sect. C: Cryst. Struct. Commun. **54**, 2 (1998).

¹⁹S. Geupel, K. Pilz, S. van Smaalen, F. Buellesfield, A. Prokofiev, and W. Assmus, Acta Crystallogr., Sect. C: Cryst. Struct. Commun. **58**, i9 (2002).0108-2701

²⁰C. Calvo, Inorg. Chem. **7**, 1345 (1968).

²¹S. Boudin, A. Grandin, M. M. Borel, A. Leclaire, and B. Raveau, Acta Crystallogr. C **49**, 2062 (1993).0108-2701

²²K. Y. Leung and C. Calvo, Can. J. Chem. **50**, 2519 (1972).